Virchows Arch (1995) 426:509–517

ORIGINAL ARTICLE

Sibylle Tenschert · Marlies Elger · Kevin V. Lemley

Glomerular hypertrophy after subtotal nephrectomy: relationship to early glomerular injury

Received: 30 December 1994 / Accepted: 6 March 1995

Abstract Structural adaptations in response to approx. 70% nephrectomy were studied in male Sprague-Dawley rats. Rats developed systemic hypertension as well as progressive albuminuria after nephrectomy. At 18–26 weeks after nephrectomy (n=6) or sham treatment (n=6) kidneys were perfusion-fixed and examined by light and electron microscopy. Glomerular tuft volume (+140%), capillary volume (+151%) and length (+77%), mesangial volume (+115%), podocyte volume (+96%), glomerular basement membrane surface area (+107%) and filtration slit length (+85%) were all significantly greater in nephrectomized rats. The incidence of segmental glomerular sclerosis was low and variable among these rats, but was significantly higher than in controls (P=0.037). Urinary albumin excretion was elevated in the nephrectomized rats (89±72 SD mg/day vs 11±11 mg/day in control rats, P=0.01) and correlated significantly with the incidence of sclerosis (r=+0.8311, P<0.05). The relationships of the level of albuminuria and the sclerosis rate to various morphometric parameters were examined by regression analysis for the nephrectomy group. A significant negative correlation was found between albuminuria and average tuft volume (r=–0.8136) and glomerular basement membrane surface area (r=–0.8168). Both sclerosis rate and albuminuria showed negative correlations with filtration slit length (r=–0.8180 and r=–0.8598). These findings suggest that under some circumstances, glomerular hypertrophy may prevent or ameliorate the early stages of glomerular injury after subtotal nephrectomy.

K. V. Lemley (✉)[1]
Departments of Pediatrics and Physiology,
West Virginia University School of Medicine,
Morgantown WV 26506, USA

M. Elger · S. Tenschert · K. V. Lemley
Institute of Anatomy and Cell Biology I, University of Heidelberg,
D-69120 Heidelberg, Germany

Mailing address:
[1] Division of Pediatric Nephrology, Room G 306
Stanford University School of Medicine,
Stanford, CA 94305-5119 USA

Key words Morphometry · Stereology · Focal glomerular sclerosis

Introduction

Functional adaptations to the acute loss of renal mass begin within hours [17]. Structural adaptations begin to occur within days [26]. Evidence of glomerular dysfunction following partial renal ablation is also apparent quite early – in the form of proteinuria. The level of proteinuria correlates with the rate of progression of disease in patients [25] and probably also in experimental animals. Inasmuch as structurally "intact" nephrons [27] – i.e. those without evidence of glomerular sclerosis – are probably the main source of proteinuria in remnant kidneys, it seems likely that the same early hemodynamic and structural adaptations which lead to proteinuria in *nonsclerotic* glomeruli underlie the development of later structural glomerular injury. This study employs morphometric techniques to characterize some of the structural adaptations in nonsclerotic hypertrophic glomeruli 18 weeks after subtotal nephrectomy in male Sprague-Dawley rats and compares glomeruli in these animals with those in normal controls.

A common feature of experimental models of glomerular sclerosis is a heterogeneity in the degree of glomerular damage found in identically treated animals – as manifested, for example, in variable rates of proteinuria and of segmental glomerular sclerosis (SGS) [7]. Differences in the early structural and functional adaptations to the loss of renal mass may in fact influence the degree or tempo of subsequent glomerular injury. We therefore used correlation analysis within the nephrectomy group in order to determine which *structural* characteristics of the hypertrophic process were associated with the early development of glomerular damage in the remnant nephron population.

Materials and methods

Animals

Male Sprague-Dawley rats (body weight 215–252 g) were used. After a 24-h urine collection in metabolic cages, they underwent either subtotal nephrectomy (NX, n=6) or control treatment (CON, n=6). Control and NX rats formed the control groups in an earlier study [9]. In the nephrectomy group, after anesthesia with pentobarbital (60 mg/kg BW i.p., Rousselot, Paris, France), the right kidney was removed in toto and all visible extrarenal branches of the left renal artery were ligated, with exception of the most posterior branch. As estimated by cortical discoloration, this resulted in approximately 72% reduction (range, 67–80%) in functional renal mass. Silk (5–0) or cotton (6–0) thread was used for the ligation so that vessel closure was complete. With synthetic suture, there may be transient cortical ischemia at the time of ligation owing to reversible vasospasm, but if vessel closure is only partial, areas of renal hypoperfusion – rather than infarction – may result. All nephrectomies were performed by the same investigator in order to assure technical uniformity. Controls underwent pentobarbital anesthesia and jugular vein catheterization with infusion of 1.0 ml of normal saline (these rats were controls in a multi-treatment study, in which some experimental animals underwent subtotal nephrectomy while others received intravenous infusions of various drugs).

After recovery, the animals were maintained on an ad lib diet of standard rat chow (ssniff R, with 21% protein, 0.45% Na^+ content; ssniff Spezialfutter GmbH, Soest, FRG). Urinary albumin excretion was determined periodically by single radial immunodiffusion as previously described [9]. In 10 of the rats (6 NX, 4 CON), systolic blood pressure was determined during the first 8 weeks after treatment, using the tail-cuff method in a light ether-anesthetized state. After 18 weeks all NX and 2 control rats were anesthetized with thiobarbiturate (100 mg/kg BW, i.p., Byk) and the kidneys were perfusion fixed by standard procedures [9]. The remaining 4 controls were prepared identically 8 weeks later, i.e. 26 weeks after sham treatment. All experiments were conducted in accordance with the NIH "Guide for the Care and Use of Laboratory Animals" and the "German Law on the Protection of Animals."

Histology

Paraffin-embedded coronal slices of the kidneys were cut at 2 μm, stained by the periodic acid Schiff reaction (PAS) technique and used for determination of glomerular tuft volume (see "Morphometric studies" below) and for pathological evaluation. Tissue from the previous study [9] was reprocessed (embedded, cut and stained) for use in this study. For determination of the sclerosis rate, glomeruli in 2–4 kidney slices (>200 μm apart) from each rat were scored in random order and independently by two observers unaware of the identity of the sections. From 250 to 761 glomeruli were evaluated in each of the control animals. In NX rats, 210–540 glomeruli were evaluated from each animal. The percentage of glomerular profiles not directly adjacent to a region of interstitial scarring and showing segmental glomerular sclerosis (SGS) – as evidenced by either synechiae or segmental capillary collapse with hyalin deposition – was determined. Regions of interstitial scarring were minimal in both CON and NX animals. Glomeruli with SGS were distinguished from those showing ischemic collapse [12] (Fig. 1A, B), which was present in both groups in similar frequencies outside of regions bordering infarcted tissue (CON=1.5±0.8 SD%; NX=1.3±0.6%). The incidence of segmental sclerosis was determined in glomeruli from the entire cortex (not just superficial glomeruli).

Cortical tissue was post-fixed in a low-osmium (0.1%) solution, followed by tannic acid and uranyl acetate, cold dehydration in acetone, and embedding in Epon [19]. Ultrathin sections for morphometric analysis were examined by electron microscopy (Philips 301).

Morphometric studies

Tuft areas (minimal inscribing polygon) were determined in 100 nonsclerotic superficial glomerular profiles per rat from the 2-μm paraffin sections using a semiautomatic image analysis system (VIDS IV, AiTectron, Düsseldorf, Germany). Average tuft area $\bar{A}_t$ was used to calculate an average tuft volume for each animal: $\bar{V}_t=(\beta/k) \cdot (\bar{A}_t)^{3/2}$, where β=1.38 (shape coefficient for spherical particles) and k=1.1 (size distribution coefficient) [23]. Average tuft volume was corrected for the effects of shrinkage during paraffin embedding [1].

For the measurements at the EM level, all glomeruli in a section from an Epon block, which lay within the first three superficial glomerular layers (within circa 1200 μm of the kidney surface) and which showed no evidence of sclerosis were photographed (×570). This often required several ultrathin sections to be examined before a given glomerulus could be found entirely between grid bars (50 mesh copper grids). Subsequently, single-hole grids were used to avoid this problem. This procedure was repeated on additional blocks until 10 glomeruli were photographed. If the number of glomeruli in the final block would have brought the total number for that animal to more than 10, glomeruli to be photographed were selected by lots *before* electron microscopy. In this way, all glomerular profiles appearing in the sections were equally likely to be included in the morphometric evaluation, regardless of their size. Both exclusion of smaller glomerular profiles and an unconscious selection bias against the largest profiles (which fall on grids more often than smaller ones) can influence the results of the morphometric analysis (unpublished observations). The glomerular profiles were photographed in their entirety and photomontages were made for analysis at a final magnification of ×1840.

Tuft polygonal area, the area enclosed by glomerular basement membrane (GBM), capillary lumen area (including endothelium), GBM length and pericapillary GBM length were determined by planimetry. Pericapillary GBM was considered to be that part of the GBM overlying endothelial cells (either the fenestrated part or the perikaryon). Perimesangial GBM length for each profile was calculated as the difference between total GBM length and pericapillary GBM length. Mesangial area was calculated as the difference between GBM-included area and capillary area. Total podocyte area and podocyte nuclear area were determined by point counting. The number of podocyte nuclear intersections in each glomerular montage was determined by consensus of at least two observers. Corresponding volume (V_V), area (S_V), length (L_V), and number (N_V) densities (per unit tuft volume) for the various glomerular components were calculated using standard morphometric formulas [23]. Absolute values of the tuft components were determined as the product of the various densities with the average tuft volume, $\bar{V}_t$.

In addition, total glomerular filtration slit length was estimated. Higher-power photomicrographs (×3420) were made randomly in all NX and in 2 CON rats from a subset of the same glomeruli represented by the above-mentioned photomontages. The number of filtration slit intersections per unit tuft polygonal area (N_A) was determined and the slit length density was calculated as $L_V = 2 \cdot N_A$ [23].

Parameters describing conformation of pericapillary GBM and tuft

The average surface curvature of the pericapillary GBM was determined by two different methods. First, a modification of the method published by Seyer-Hansen et al. [20] ("capillary tube method") was used. This method calculates the average glomerular capillary radius from the average capillary lumen cross-sectional area; the latter is estimated as the total capillary volume divided by the total capillary length.[1] The second method for determining the GBM curvature is model-independent and is based on a stereo-

[1] The radius provides an estimate of only one of the two principal curvatures of the endothelial tube surface [10]. If the other principal curvature is neglected (i.e., if the axial bend in the endothelial tube is assumed to be negligible in comparison with the radial curvature component), the average mean surface curvature $\bar{K}$ [23] of the capillary endothelial tube may be estimated by dividing the reciprocal of the tube radius by 2: $\bar{K}=\sqrt{\Pi} \cdot N_A/2 \cdot A_A$ where N_A is the number of capillary lumen intersections per unit tuft area and A_A is the areal density of capillary lumen per tuft area

logic relation between the average *lineal* curvature $\bar{C}$ of the intersection of the membrane with a sectioning plane and the average mean *surface* curvature $\bar{K}$ of the membrane in 3D space: $\bar{K}=(\pi/4)\cdot\bar{C}$ [23]. Average lineal curvature was determined from digitized coordinate data of the individual segments of pericapillary GBM. The data were first smoothed to remove tracing and digitization artifact, using a 2-dimensional adaptation of the robust locally weighted regression technique (LOWESS) for time series data [3].

In addition to these standard stereologic parameters, a quantitative index of tuft form (folding index) was calculated for each animal:

$$\mathbf{F}=6\cdot\sqrt{\pi}\cdot(\text{GBM-included volume})/(\text{GBM surface area})^{3/2}$$

This is simply the ratio of the estimated GBM-included volume to the maximum volume which the GBM would contain, were it to be completely "unfolded" (i.e. blown up into a sphere). Thus, the smaller the value of this index, the more highly folded the GBM is.

Fig. 1A, B Light micrographs of glomeruli manifesting (A) segmental glomerular sclerosis and (B) ischemic collapse. The glomerular profile in A shows a large adhesion (*arrows*) opposite the vascular pole. Outside the area of the adhesion, the capillary loops are patent and the mesangium shows only mild expansion. The ischemic glomerular profile (to the *left* in B) is shrunken throughout, with uniformly small but patent capillary lumina, a very small Bowman's capsule and a thickened parietal layer. (PAS, ×300; *bar* 50 μm)

Fig. 2 Development of albuminuria in individual NX rats. Note the consistency of the relative severity of albuminuria over most of the study period. Each rat seems to find its own "trajectory" early in the study. The trajectories of individual rats in general do not cross

Statistical analysis

Interval data are reported as mean±SD. Unpaired comparisons between groups were made using Student's *t*-test or the Mann-Whitney test [6]. Slopes of regression lines were analyzed by *t*-test [15]. Since many of the relationships between morphometric variables and the level of albuminuria appeared to be exponential rather than linear in nature, these correlations were analyzed by exponential regression [15]. The NCSS software package (Unisoft, Augsburg, Germany) was used for some of the calculations. The associations of albuminuria and sclerosis rate with the morphometric variables were also examined by multiple regression (stepwise and forward selection procedures).

Results

Whole animal data

Body weight increased equivalently in nephrectomy and control groups (final BW: 544±40 g, NX; 589±43 g, CON). By 8 weeks after nephrectomy systolic blood pressure was significantly higher in NX than in controls (220±21 mmHg, n=6; 129±14 mmHg, n=4, P=0.01). Albuminuria also increased progressively over baseline values (<1 mg/day) in both NX and CON. Final measured urinary albumin excretion rates were 89±72 mg/day in NX and 11±11 mg/day in CON (NX vs CON: P=0.01). Despite significant variability in the severity of albuminuria among the NX rats, each rat appeared to follow its own individual trajectory for the development of albu-

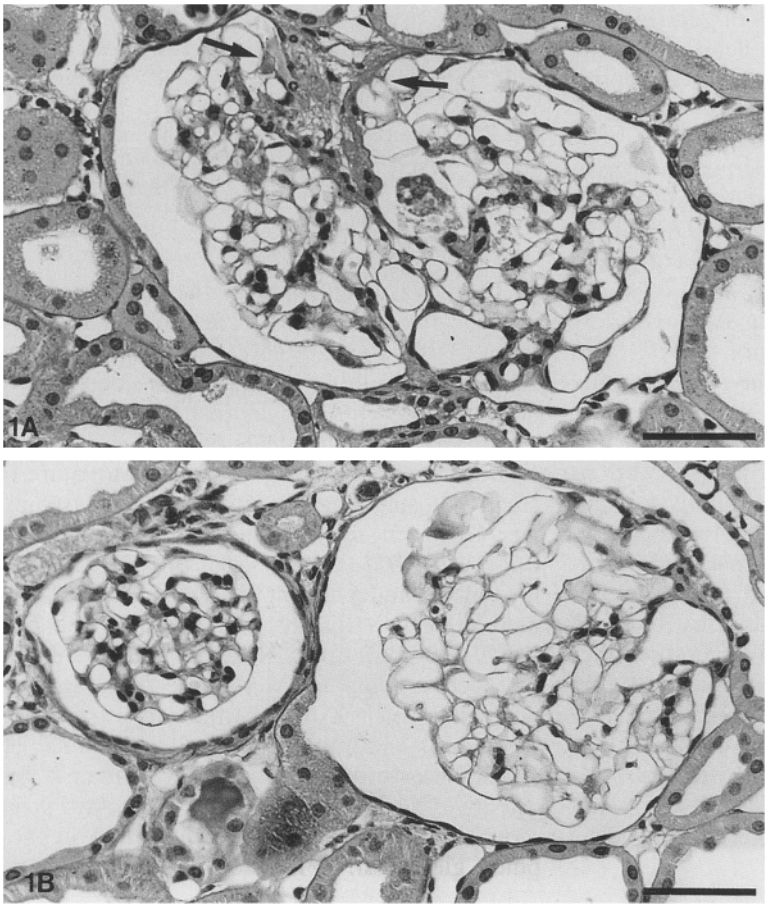

minuria (Fig. 2). The final rank order of albuminuria among NX (at 17 weeks) was already apparent 9 weeks after nephrectomy, when levels of albuminuria were still relatively modest. A similar phenomenon with respect to the development of the usual age-related albuminuria was seen in controls (data not presented).

Dimensions of glomerular damage and hypertrophic response

At the time of perfusion fixation, the remnant kidneys of NX rats were massively hypertrophied. Histologically, few glomeruli not directly adjacent to areas of ischemic scar showed SGS in NX (highest incidence 1.64%), despite the occurrence of systemic hypertension by 8 weeks after subtotal nephrectomy and significant levels of albuminuria at the time of perfusion fixation. The profiles of hypertrophied glomeruli had open capillary loops (Fig. 3) and less than 6% of such glomeruli showed mesangial expansion. In general, few interstitial changes (fibrosis, cellular infiltrates) were seen, except bordering areas of ischemic scar. Almost no areas of denuded GBM were observed. The true incidence of SGS was probably greater than Table 1 indicates, since the frequencies of segmental lesions are systematically underestimated by analysis of single histological sections. Remuzzi et al. [18] have estimated the true incidence of SGS to be about 3 times that determined from single histological sections. In addition, we excluded both sclerotic glomeruli directly adjacent to regions of scarring and glomeruli showing ischemic collapse in determining the number of glomeruli with segmental sclerosis. In control rats, SGS was in fact extremely rare: only 2 of 2227 glomerular profiles manifested segmental sclerosis.

Thus, despite their relatively good structural preservation, NX rats still had a significantly higher incidence of SGS than CON: 0.80±0.65% vs. 0.10±0.17% (P=0.037). In addition, the incidence of SGS among NX correlated well with the level of albuminuria at 17 weeks (r=+0.8311, P<0.05; Fig. 4), suggesting that even low levels of SGS reflect true glomerular injury.

All individual tuft components displayed substantial hypertrophy after NX, albeit to somewhat different degrees (Tables 2, 3). GBM-included volume (+144%) and capillary volume (+151%) grew more or less proportionately. Mesangial volume (+115%) also increased, although less than total capillary volume, for example. Thus, neither morphometry nor light microscopic examination revealed evidence of "pathologic" mesangial expansion. Total GBM surface area increased by 107% in NX: pericapillary GBM increased by 114% and perimesangial GBM by 91%. Filtration slit length increased by 85%. The width of the filtration slits did not appear to differ appreciably between NX and CON, or among NX (data not shown). Podocyte volume increased by 96%. Total capillary length increased less (+77%), implying an increase in capillary cross-sectional area (inasmuch as total capillary volume rose by +151%).

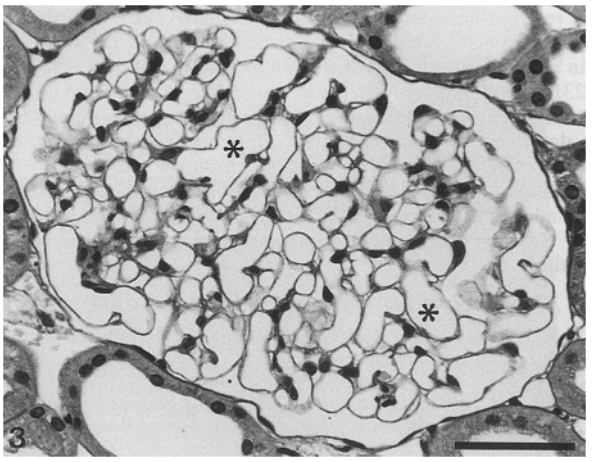

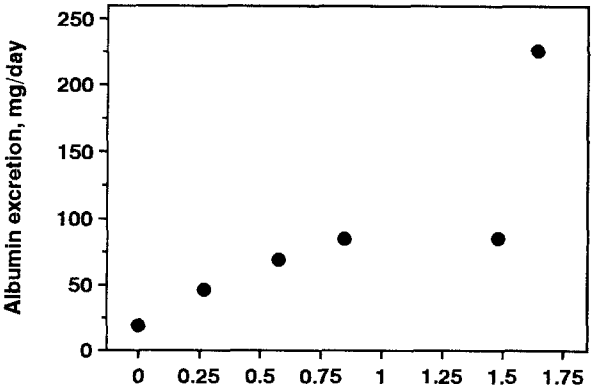

Fig. 4

Fig. 3 Micrograph of a massively hypertrophied glomerulus 18 weeks after 3/4 nephrectomy. Note the open capillary loops and narrow mesangium. Some capillary loops (*asterisks*) are widened. (PAS, ×300; *bar* 50 μm)

Fig. 4 Relationship between albuminuria and segmental glomerular sclerosis (SGS) in NX rats. The two variables correlate strongly with each other (r=+0.8311, P<0.05), despite the low incidence of SGS

There was a tendency for the number of podocyte nuclei per glomerulus to be greater after subtotal nephrectomy (310±48 vs 249±56, P=0.07), although values for NX and CON rats overlapped considerably. Whether or not this represents true cellular hyperplasia is unclear inasmuch as a few binucleate podocytes were seen.

Both measures of GBM surface curvature indicated a small but statistically significant decrease in pericapillary GBM surface curvature in NX rats (0.0873±0.0067 μm^{-1} vs 0.1011±0.0051 μm^{-1} in CON, P=0.0025, using the model-independent method). The capillary tube method gave slightly larger values in both groups (0.1011±0.0052 μm^{-1}, NX; 0.1198±0.0058 μm^{-1}, CON). The pericapillary GBM thus became larger and somewhat flatter in NX rats. At the same time, the glomeruli in NX rats had not simply "ballooned out." The folding index F was even lower in NX rats than it was in CON (0.0269±0.0012 vs 0.0334±0.004, P<0.01), indicating a more highly folded form of the GBM in the hypertrophied glomeruli. It is also clear from the micrographs

Table 1 Average (mean ± SD) group values for control and NX rats. (*BW* Body weight at time of nephrectomy or sham treatment (*BW-1*) and at time of perfusion fixation (*BW-2*), *Syst. BP* systolic blood pressure 8 weeks after NX or sham treatment, $U_{alb}V$ urinary albumin excretion, *SGS* incidence of segmental glomerular sclerosis, $\bar{V}_t$ average glomerular tuft volume.)

Group	BW-1 (g)	BW-2 (g)	Syst. BP (mm Hg)	$U_{alb}V$ (mg/d)	SGS (%)	$\bar{V}_t$ ($\mu m^3 \times 10^6$)
CON (n=6)	244±7	589±43	129±14 (n=4)	11±11	0.10±0.17	2.59±0.28
NX (n=6)	237±13	544±40	220±21* (n=6)	89±72*	0.80±0.65**	6.22±0.63***

*P=0.01; **P<0.05 (Mann-Whitney test); ***P<0.0001 (Student's t-test)

Table 2 Morphometry of tuft components (1). ($\bar{V}_{GBMincl}$ average glomerular volume included by GBM, $\bar{V}_{cap}$ capillary volume per glomerulus, $\bar{V}_{podo}$ total podocyte volume per glomerulus, $\bar{V}_{mes}$ mesangial volume per glomerulus, $\bar{S}_{pcGBM}$ pericapillary GBM surface area, $\bar{S}_{pmGBM}$ perimesangial GBM surface area.)

Group	$\bar{V}_{GBMincl}$ ($\mu m^3 \times 10^6$)	$\bar{V}_{cap}$ ($\mu m^3 \times 10^6$)	$\bar{V}_{podo}$ ($\mu m^3 \times 10^6$)	$\bar{V}_{mes}$ ($\mu m^3 \times 10^5$)	$\bar{S}_{pcGBM}$ ($\mu m^2 \times 10^5$)	$\bar{S}_{pmGBM}$ ($\mu m^2 \times 10^5$)
CON (n=6)	1.422±0.116	1.147±0.093	0.586±0.126	2.752±0.360	4.058±0.465	1.892±0.337
NX (n=6)	3.475±0.517*	2.882±0.382*	1.146±0.127**	5.924±1.602*	8.707±0.758**	3.617±0.384**
Δ%	+144%	+151%	+96%	+115%	+114%	+91%

*P<0.005 (Mann-Whitney test); **P<0.0001 (Student's t-test)

Table 3 Morphometry of tuft components (2). ($\bar{L}_{cap}$ total capillary length per glomerulus, $\bar{L}_{filt}$ total filtration slit length per glomerulus, $\bar{N}_{podo}$ average number of podocytes per glomerulus, $\bar{K}_{pcGBM}$ average mean surface curvature of the pericapillary GBM based on the average lineal curvature, $\bar{K}_{etub}$ average mean surface curvature of the capillary endothelial tube based on the tube method and corrected for the second principal curvature of the surface, *F index* folding index of GBM.)

Group	$\bar{L}_{cap}$ ($\mu m \times 10^4$)	$\bar{L}_{filt}$ ($\mu m \times 10^6$)	$\bar{N}_{podo}$ (#/glom)	$\bar{K}_{pcGBM}$ ($\mu m^{-1} \times 10^{-1}$)	$\bar{K}_{etub}$ ($\mu m^{-1} \times 10^{-1}$)	F index ($\times 10^{-2}$)
CON (n=6)	2.108±0.331	1.366±0.108 (n=2)	249±56	1.011±0.051	1.198±0.058	3.340±0.398
NX (n=6)	3.730±0.315*	2.533±0.321 (n=6)	310±0.48**	0.873±0.067*	1.011±0.052*	2.692±0.123***
Δ%	+77%	+85%	+24%	−13.6%	−15.6%	−19.4%

*P≤0.0025; **P=0.07 (Student's t-test); ***P<0.01 (Mann-Whitney test)

that the tufts had not lost their structural complexity with hypertrophy (Fig. 3).

Correlation analysis among the NX rats

Despite identical treatment and grossly identical degrees of hypertrophy of the remnant kidneys, there was a wide spectrum in the degree of glomerular injury in the NX group: urinary albumin excretion ranged from 18.7 to 226 mg/day and the incidence of SGS in the histological sections varied from 0 to 1.64%. One NX rat, despite having undergone an estimated 75% renal ablation and showing massive glomerular hypertrophy (estimated $\bar{V}_t$ equal to 280% of average control tuft volume), actually had a lower rate of albuminuria and SGS than two of the controls. This large variation in the level of glomerular injury allowed us to examine by correlation analysis those structural features of the hypertrophic response in remnant glomeruli that may have influenced the severity of early glomerular injury. Both albuminuria and the rate of SGS were used as measures of glomerular injury. The significant correlation (r=+0.8311, P<0.05; see Fig. 4) between SGS and albuminuria supports the proposition that these two variables reflect different aspects of a single injury process. Although the populations of glomeruli which manifest SGS and those which contribute most significantly to albuminuria probably bear a relationship to each other, they are not the same, since the major source of albuminuria is structurally intact glomeruli [27].

Albuminuria at 17 weeks correlated *negatively* with glomerular tuft volume (r=–0.8136, by exponential regression; P<0.05; Fig. 5) and GBM-included volume (r=–0.8433, P< 0.05). Among the individual tuft components showing significant correlations with albuminuria was GBM surface area (r=–0.8168, P<0.05). A significant negative correlation also existed between albuminuria and mesangial volume (r=–0.8555, P<0.05).. The most striking observation in this study, however, was the significant negative correlation between filtration slit length and both albuminuria and SGS (r=–0.8598 and r=–0.8180, respectively; P<0.05; Fig. 6A, B). There were no statistically significant *positive* correlations of individual tuft components with albuminuria and SGS.

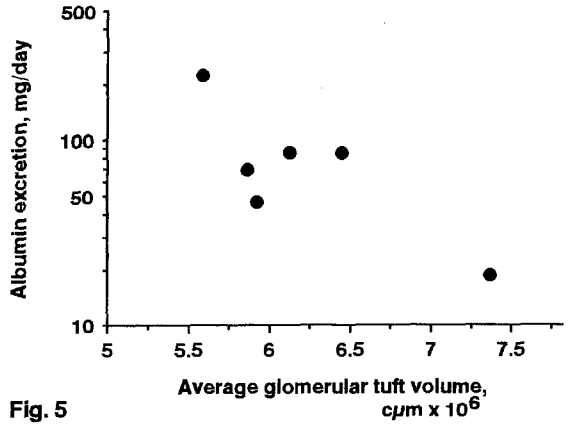

Fig. 5

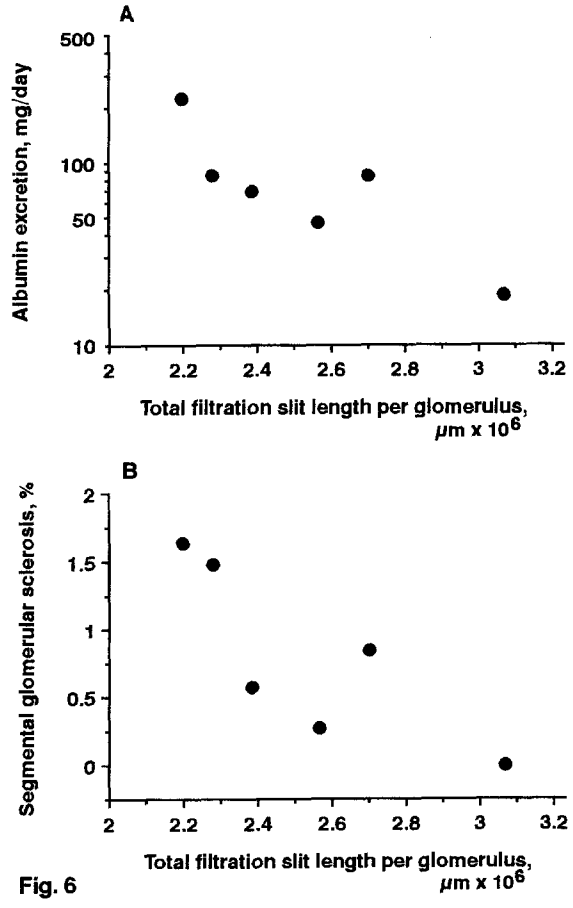

Fig. 6

Fig. 5 Relationship of albuminuria to average glomerular tuft volume in NX rats (r=–0.8136, P<0.05). Albuminuria is lowest in the rat with the greatest degree of hypertrophy

Fig. 6 **A** Relationship of albuminuria to total filtration slit length per glomerulus (r=–0.8598, P<0.05). **B** Relationship of SGS to total filtration slit length per glomerulus (r=–0.8180, P<0.05)

Multilinear regression analysis[2] was performed using log(albuminuria) and SGS as dependent variables and GBM surface area, pericapillary GBM surface area, filtration slit length, mesangial volume and number of podocytes as independent variables. This analysis showed slit length to be a significant predictor for both albuminuria and SGS by both stepwise and forward procedures (P=0.0281 for albuminuria; P=0.0466 for SGS). In the forward procedure, pericapillary GBM area also entered significantly into the model (P=0.2821; R^2 value increased from 0.6695 to 0.7895 when this variable was added to slit length).

We examined two specific *structural* mechanisms that have been proposed to account for the development of SGS in hypertrophied glomeruli: podocyte "insufficiency" [5] and increased capillary wall tension due to decreased capillary wall curvature as described by the Young-Laplace relation [4]. In an attempt in find a quantitative, stereologic basis for the concept of podocyte insufficiency, the correlations of albuminuria and SGS with the total number and number density of podocytes, the number of podocytes per unit GBM surface area and the total podocyte cell volume per unit GBM surface area were examined. None showed a significant correlation, although the number of podocyte nuclei demonstrated a tendency toward a negative correlation with albuminuria (r=–0.5120, P≅0.30).

With respect to the effects of GBM wall tension on glomerular injury, there was no significant correlation between either SGS or albuminuria and GBM surface curvature (r=+0.3370 and r=+0.5013, P=NS). Thus, neglecting the influence of the transmural hydrostatic pressure difference on wall tension, from a purely morphologic standpoint, increased wall tension (i.e. that due to decreased GBM curvature) had *no* deleterious effect on the glomeruli. There was no statistically significant correlation of either injury variable with systemic blood pressure, although it must be borne in mind that this parameter was last measured 8 weeks after subtotal nephrectomy.

Discussion

The purpose of this study was to develop a morphometric characterization of the process of glomerular hypertrophy that might yield insight into those structural factors of the adaptive process that influence the development of SGS after reduction of renal mass. To this end, a number of morphometric features in hypertrophied glomeruli were correlated with quantitative measures of glomerular injury (albuminuria, frequency of glomeruli showing segmental glomerular sclerosis).

There have been several earlier morphometric studies of glomerular structure following subtotal nephrectomy. Olivetti et al. [14] studied male Wistar rats 5 weeks after uninephrectomy. They found increases in glomerular capillary volume and total capillary length roughly proportionate to the change in tuft volume, and an increase in mesangial volume (matrix and cells) that slightly exceeded the increase in $\bar{V}_t$. Shea et al. [21] found results similar to ours in their 5/6 nephrectomy model in female Sprague-Dawley rats. The degree of tuft hypertrophy at 18 weeks was roughly the same (+156% vs +140%) in

[2] Use of log (albuminuria) is equivalent to performing exponential regression on albuminuria. Tuft volume was not included as an independent variable in the analysis, inasmuch as the other morphometric parameters are all dependent on the tuft volume

the present study, as was the change in pericapillary GBM surface area (95% vs 114%). Filtration slit length, on the other hand, increased by only 45% (vs 85% in our study). In neither of these earlier studies [14, 21] were the morphometric indices correlated with measures of glomerular injury.

Glomeruli of NX rats in this study differed from those of controls in every structural parameter measured. There was heterogeneity in the magnitude of the hypertrophic response among the different tuft compartments, but in general the degree of hypertrophy was massive (e.g. tuft volume 2½ times as large as control tufts). This degree of hypertrophy is somewhat greater than that seen after 3/4 or 5/6 nephrectomy in Wistar rats [2, 5], but is comparable to the degree of hypertrophy following 5/6 nephrectomy in female Sprague-Dawley rats [21]. Capillary volume increased more than any other compartment. In contrast, growth of the mesangium after NX was proportionately less than overall tuft growth. Thus, we found mesangial hypertrophy rather than mesangial "expansion." In addition, a high degree of complexity of tuft form was preserved despite significant hypertrophy (Fig. 3).

Within the NX group, there was considerable variability both in the level of glomerular injury (as reflected in albuminuria and SGS) and in the quantitative indices of glomerular hypertrophy. This allowed these signs of glomerular damage to be correlated with changes in glomerular structure at the level of individual animals. That some feature of the early adaptive response to the loss of renal mass led to later glomerular injury is suggested by examination of the time-course of albuminuria (Fig. 2), which suggests a progressive process with the relative severity in individual rats established quite early. Three weeks after NX, for example, the rat that would have the highest level of albuminuria and sclerosis rate at the end of the study already had clearly more albuminuria than the others in its cohort.

The low incidence of SGS 18 weeks after NX was unexpected. For example, one NX rat had no sclerotic glomerular profiles (0/268) on histological examination despite massive glomerular hypertrophy and significant hypertension (200 mmHg) 8 weeks after NX. Even allowing for undercounting of sclerotic lesions because single histological sections had been used [18], the maximum incidence of SGS in the NX group was certainly less than 10%. We did not include glomeruli showing ischemic collapse (Fig. 1B) in the calculation of the incidence of SGS. It is likely that the pathogenesis of the former lesion is distinct from that of SGS [12]. In addition, we did not include sclerotic glomeruli abutting regions of scarring. Local factors, such as inflammatory mediators or the impingement of scar tissue on the vasculature, might have contributed to injury in such glomeruli. In this study, we wished to examine the influence of glomerular hypertrophy itself on the development of segmental glomerular injury.

Even allowing for our rigorous inclusion criteria, the incidence of SGS in our study may have been lower than that in other studies. For example, the sclerosis rate varied from about 1% to 11% by 11 weeks after 3/4 nephrectomy in the study of Fries et al. [5]. Although terminating our study later would have resulted in higher rates of segmental sclerosis, the pathogenetic mechanisms leading to glomerular damage were probably in effect from a quite early stage. It seems very likely that the rats with the highest sclerosis rates and quantitatively greatest albuminuria at 17–18 weeks would have been the most severely affected in subsequent weeks. Examining the relationship of glomerular injury to the various morphometric indices early in the course allows us to examine those morphological adaptations that put the remnant glomeruli most at risk of subsequent injury.

The principal – and unexpected – finding of this study is that glomerular damage 18 weeks after subtotal nephrectomy correlates negatively with several indices of tuft hypertrophy. Two studies have provided evidence for a *positive* relationship between glomerular size and SGS after NX by correlation analysis [5, 26]. Both studies were performed in Wistar rats. Other studies have either failed to show such a relationship [2, 7, 8, 11, 22] or have compared only group averages of glomerular size and sclerosis rate [4, 13]. By analysis of group averages alone, we would also have found a positive "association" between tuft volume and glomerular damage. It is preferable to use correlation analysis when examining a multifactorial process such as the development of SGS, however. That some consequence of NX accelerates the development of sclerosis in the remnant glomerular population seems beyond dispute. A correlation analysis is necessary to determine which specific features of the hypertrophic process influence the underlying pathogenetic mechanism and to avoid spurious associations.

Our results do not support an obligatory role for glomerular hypertrophy in the development of progressive glomerular injury. Although a number of earlier studies [2, 8, 11, 22] have called in question a causal association of glomerular hypertrophy per se with glomerular sclerosis, this is the first study to present evidence suggesting a *protective* effect of hypertrophy. In fact, one mechanism by which an increase in tuft size (more particularly, in filtration surface area) might be protective in the setting of reduced renal mass can be suggested immediately. If despite adaptive hyperfiltration, the rate of glomerular filtration at the single nephron level is still under feedback control in the weeks following 3/4 nephrectomy – as it is 4–6 weeks after 1+1/3 NX [16] and 8 weeks after 3/4 NX [24] – then an increase in effective filtration surface area would probably limit the increase in P_{GC} required to attain the set-point single nephron GFR. In our study, the increase in filtration surface area (85% for filtration slit length) represents a significant *structural* mechanism facilitating an increase in nephron filtration rate, particularly in the setting of filtration pressure disequilibrium.

In our analysis, we addressed two specific mechanisms by which glomerular hypertrophy has been proposed to influence the development of glomerular sclerosis: increases in capillary wall tension [4] and podocyte "insufficiency" [5]. As expected, pericapillary GBM cur-

vature is decreased in NX animals; this should contribute to increased capillary wall tension. The lack of a significant correlation between GBM curvature and indices of glomerular injury among the NX rats, however, suggests that in this model capillary wall curvature is not a decisive factor in the development of glomerular injury. Nevertheless, conclusive statements regarding capillary wall tension cannot be made in the absence of measurements of both wall curvature and transmural pressure gradients, which together determine the wall tension.

With regard to a role for podocyte insufficiency, there was suggestive evidence that an increase in the number of podocytes may be associated with relative glomerular preservation. This contrasts with the findings of Fries et al. [5], who found no evidence for an increase in podocyte number following subtotal nephrectomy in Munich-Wistar rats. The fact that they described, in addition, a positive association between tuft volume and sclerosis rate suggests that the podocyte may be a pivotal factor in determining the susceptibility of hypertrophic glomeruli to injury and supports the idea that an inadequate number of podocytes may be a major risk factor for the development of SGS. The strong negative correlation of total filtration slit length with both indices of glomerular injury suggests that the role of the podocyte in the formation of filtration slits may explain the importance of an adequate number of podocytes to the structural preservation of the hypertrophic glomerulus. Simplification of foot processes as a result of podocyte cellular injury (e.g. toxic injury due to Adriamycin) would also cause a relative decrease in the total length of filtration slits in the tuft and has been shown to be an aggravating factor under these circumstances [5]. If the number of podocytes is inadequate to cover an expanded GBM, filtration slit density may fall and with it the ultrafiltration coefficient. Intraglomerular pressures would thereby have to rise as a compensatory response, accelerating capillary injury and the development of segmental sclerosis.

The following interpretation of our data is offered. Glomerular hypertrophy is a state of heightened structural stress [10]. If it occurs without either a loss of structural stability or significant foot process simplification, it may actually preserve glomerular function in the face of the need for increased single nephron filtration – by increasing filtration surface area, thereby limiting the adaptive increase in glomerular capillary pressure otherwise required to attain an elevated SNGFR. The ability of the podocytes to respond to increased glomerular filtration demands by forming filtration slits will help to determine the intracapillary pressure in the glomerulus. Inadequate expansion of the effective filtration surface – due to podocyte "insufficiency" – may contribute to glomerular capillary hypertension, accelerating the development of segmental sclerosis.

Acknowledgements Portions of this work were presented at the XIIth International Congress of Nephrology, Jerusalem (June 1993). This study forms part of Ms. Tenschert's dissertation for the degree of Doctor of Medicine from the University of Heidelberg. During part of this study, Dr. Lemley was a fellow of the Alexander von Humboldt Foundation. The expert technical assistance of Ms. Bruni Hähnel and Ms. Ingrid Hartmann is gratefully acknowledged. We thank Drs. T. H. Hostetter and C. Baylis for useful comments.

References

1. Bankir L, Fischer C, Fischer S, Jukkala K, Specht HC, Kriz W (1988) Adaption of the rat kidney to altered water intake and urine concentration. Pflügers Arch 412: 42–53
2. Bidani AK, Mitchell KD, Schwartz MM, Navar LG, Lewis EJ (1990) Absence of glomerular injury or nephron loss in a normotensive rat remnant kidney model. Kidney Int 38: 28–38
3. Chambers JM, Cleveland WS, Kleiner B, Tukey PA (1983) Graphical methods for data analysis. Wadsworth International Group, Belmont, Calif
4. Daniels BS, Hostetter TH (1990) Adverse effects of growth in the glomerular microcirculation. Am J Physiol 258: F1409–F1416
5. Fries JWU, Sandstrom DJ, Meyer TW, Rennke HG (1989) Glomerular hypertrophy and epithelial cell injury modulate progressive glomerulosclerosis in the rat. Lab Invest 60: 205–218
6. Glantz SA (1981) Primer of biostatistics. McGraw-Hill, New York
7. Grond J, Goor H van, Erkelens DW, Elema JD (1986) Glomerular sclerosis in wistar rats: analysis of its variable occurrence after unilateral nephrectomy. Br J Exp Pathol 67:473–479
8. Grond J, Beukers JYB, Schilthuis MS, Weening JJ, Elema JD (1986) Analysis of renal structural and functional features in two rat strains with a different susceptibility to glomerular sclerosis. Lab Invest 54:77–83
9. Lemley KV, Kriz W (1991) Glomerular injury in analbuminemic rats after subtotal nephrectomy. Nephron 59:104–109
10. Lemley KV, Elger M, Koeppen-Hagemann I, Kretzler M, Nagata M, Sakai T, Uiker S, Kriz W (1992) The glomerular mesangium: capillary support function and its failure under experimental conditions. Clin Invest 70:843–856
11. Lombet JR, Adler SG, Anderson PS, Nast CC, Olsen DR, Glassock RJ (1989) Sex vulnerability in the subtotal nephrectomy model of glomerulosclerosis in the rat. J Lab Clin Med 114:66–74
12. Miller PL, Rennke HG, Meyer TW (1990) Hypertension and progressive glomerular injury caused by focal glomerular ischemia. Am J Physiol 259:F239–F245
13. Miller PL, Rennke HG, Meyer TW (1991) Glomerular hypertrophy accelerates hypertensive glomerular injury in rats. Am J Physiol 261:F459–F465
14. Olivetti G, Anversa P, Melissari M, Loud AV (1980) Morphometry of the renal corpuscle during postnatal growth and compensatory hypertrophy. Kidney Int 17:438–454
15. Pollard JH (1977) A handbook of numerical and statistical techniques. Cambridge University Press, Cambridge
16. Pollock CA, Bostrom TE, Dyne M, Györy AZ, Field MJ (1992) Tubular sodium handling and tubuloglomerular feedback in compensatory renal hypertrophy. Pflügers Arch 420:159–166
17. Provoost AP, Molenaar JC (1980) Changes in the glomerular filtration rate after unilateral nephrectomy in rats. Pflügers Arch 385:161–165
18. Remuzzi A, Pergolizzi R, Mauer MS, Bertani T (1990) Three-dimensional morphometric analysis of segmental glomerulosclerosis in the rat. Kidney Int 38:851–856
19. Sakai T, Kriz W (1987) The structural relationship between mesangial cells and basement membrane of the renal glomerulus. Anat Embryol 176:373–386
20. Seyer-Hansen K, Hansen J, Gundersen HJG (1980) Renal hypertrophy in experimental diabetes. Diabetologia 18:501–505
21. Shea SM, Raskova J, Morrison AB (1978) A sterologic study of glomerular hypertrophy in the subtotally nephrectomized rat. Am J Pathol 90:201–210

22. Simons JL, Provoost AP, Anderson S, Rennke HG, Troy JL, Brenner BM (1994) Modulation of glomerular hypertension defines susceptibility to progressive glomerular injury. Kidney Int 46:396–404
23. Weibel ER (1979) Stereological methods. Practical methods for biological morphometry. Academic Press, London
24. Wilke WL, Persson AEG (1992) Captopril and tubuloglomerular feedback in remnant kidneys of prehypertensive rats. J Am Soc Nephrol 3:73–79
25. Williams PS, Fass G, Bone JM (1988) Renal pathology and proteinuria determine progression in untreated mild/moderate chronic renal failure. Q J Med 252:343–354
26. Yoshida Y, Fogo A, Ichikawa I (1989) Glomerular hemodynamic changes vs. hypertrophy in experimental glomerular sclerosis. Kidney Int 35:654–660
27. Yoshioka T, Shiraga H, Yoshida Y, Fogo A, Glick AD, Deen WM, Hoyer JR, Ichikawa I (1988) "Intact nephrons" as the primary origin of proteinuria in chronic renal disease. Study in the rat model of subtotal nephrectomy. J Clin Invest 82:1614–1623